Identification of Mediator Kinase Substrates in Human Cells using Cortistatin A and Quantitative Phosphoproteomics

HHS Public Access

Author manuscript

Cell Rep. Author manuscript; available in PMC 2016 April 15.

Published in final edited form as:

Cell Rep. 2016 April 12; 15(2): 436–450. doi:10.1016/j.celrep.2016.03.030.

Identification of Mediator kinase substrates in human cells using cortistatin A and quantitative phosphoproteomics

Zachary C. Poss[1], **Christopher C. Ebmeier**[2], **Aaron T. Odell**[2,3], **Anupong Tangpeerachaikul**[4], **Thomas Lee**[1], **Henry E. Pelish**[4], **Matthew D. Shair**[4], **Robin D. Dowell**[2,3], **William M. Old**[2], and **Dylan J. Taatjes**[1,*]

[1] Department of Chemistry & Biochemistry, University of Colorado, Boulder

[2] Department of Molecular, Cell, and Developmental Biology, University of Colorado, Boulder

[3] BioFrontiers Institute, University of Colorado, Boulder

[4] Department of Chemistry and Chemical Biology, Harvard University

SUMMARY

Cortistatin A (CA) is a highly selective inhibitor of the Mediator kinases CDK8 and CDK19. Using CA, we now report a large-scale identification of Mediator kinase substrates in human cells (HCT116). We identified over 16,000 quantified phosphosites including 78 high-confidence Mediator kinase targets within 64 proteins, including DNA-binding transcription factors and proteins associated with chromatin, DNA repair, and RNA polymerase II. Although RNA-Seq data correlated with Mediator kinase targets, the effects of CA on gene expression were limited and distinct from CDK8 or CDK19 knockdown. Quantitative proteome analyses, tracking around 7,000 proteins across six time points (0 – 24h), revealed that CA selectively affected pathways implicated in inflammation, growth, and metabolic regulation. Contrary to expectations, increased turnover of Mediator kinase targets was not generally observed. Collectively, these data support Mediator kinases as regulators of chromatin and RNA polymerase II activity and suggest their roles extend beyond transcription to metabolism and DNA repair.

Graphical Abstract

*Corresponding author: Taatjes@colorado.edu.

AUTHOR CONTRIBUTIONS

CCE, ZCP, and WMO performed MS sample prep and analysis; AO and RDD analyzed RNA-seq data; TL assisted with proteome data analysis; AT, HEP, and MDS provided key reagents and advice; ZCP and DJT designed and performed experiments, analyzed data, and wrote the manuscript.

ACCESSION NUMBERS

RNA-Seq data were deposited to the Gene Expression Omnibus (GEO) with accession GSE65161 and GSE78506. Proteomics data has been deposited in the ProteomeXchange PRIDE database, identifier PXD003698.

SUPPLEMENTAL INFORMATION

Includes Supplemental Note, Experimental Procedures, four figures, and eight tables.

CONFLICT OF INTEREST

The authors declare no conflict of interest.

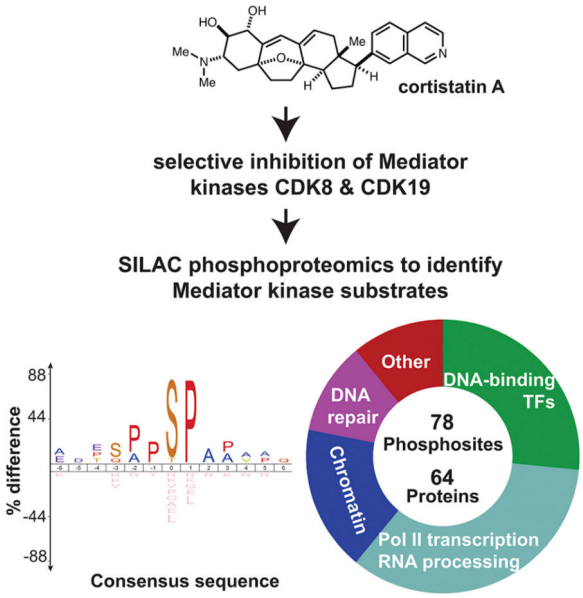

Keywords

CDK8-Mediator; Mediator; SILAC; cholesterol; MED13; MED13L; SIRT1

INTRODUCTION

An important first step in understanding the cellular function of kinases is to identify the substrates that they modify. This first step has remained a persistent challenge, in part because of the difficulties in the development of highly potent and selective kinase inhibitors. The human CDK8 kinase exists in a 600 kDa complex known as the CDK8 module, which consists of four proteins (CDK8, CCNC, MED12, MED13). The CDK8 module associates with regulatory loci on a genome-wide scale (Kagey et al., 2010; Pelish et al., 2015), and global targeting of the CDK8 module appears to reflect its association with Mediator (Allen and Taatjes, 2015). CDK19, a paralog of CDK8, emerged in vertebrates and has high sequence similarity to CDK8, including nearly identical cyclin binding and kinase domains. Comparatively little is known about CDK19; however, it appears to assemble into an analogous CDK19 module in human cells (Daniels et al., 2013).

Based upon their association with Mediator—a global regulator of RNA polymerase II (pol II) transcription—CDK8 or CDK19 may broadly impact gene expression patterns; however, physical knockdown of CDK8 or CDK19 protein levels had relatively modest effects in HCT116 cells, with 2-fold or greater changes in expression of several hundred genes (Donner et al., 2010; Galbraith et al., 2013). Whereas knockdown studies do not address the role of the kinase activity *per se*, these data suggested limited roles for the Mediator kinases in transcriptional regulation. In agreement, gene expression analyses with the CDK8 ortholog in yeast, Srb10 (Holstege et al., 1998), revealed that about 3% of genes were regulated by Srb10 kinase activity. Similarly, limited effects on yeast transcription were observed *in vitro* and *in vivo* upon selective inhibition of Srb10 (CDK8) kinase activity

using an analog-sensitive mutant (Liu et al., 2004). Most genes affected by kinase-inactive mutant Srb10 (CDK8) were involved in cellular response to nutrient stress (Holstege et al., 1998).

The biological roles of human CDK8 and CDK19 remain poorly understood, in part, because a more comprehensive identification of their substrates or the genes specifically regulated by their activities has been lacking. Our recent studies with the natural product, cortistatin A (CA), showed that CA is a potent and highly selective inhibitor of the Mediator kinases CDK8 and CDK19 (Pelish et al., 2015). CA binds the CDK8–CCNC dimer with sub-nanomolar affinity (Kd = 195 pM) and two distinct kinome profiling assays, which collectively probed approximately 400 kinases, ultimately confirmed only CDK8 and CDK19 as targets of CA, even with analyses completed at 100-times the measured IC_{50} for CDK8 (Pelish et al., 2015). Given these and other data showing the unusual selectivity of CA, we could begin to probe the cellular function and targets of CDK8 and CDK19.

Here, we report the large-scale identification of Mediator kinase (CDK8 and CDK19) substrates in human cells, using SILAC-based phosphoproteomics. We couple these results with global analysis of gene expression changes (RNA-Seq) that result from targeted inhibition of Mediator kinase activity. Furthermore, we assess potential Mediator kinase effects on protein turnover using quantitative proteomic analyses across 6 time points spanning 24 hours of Mediator kinase inhibition. HCT116 cells were chosen for this study for several reasons. First, although CA potently inhibits Mediator kinase activity in HCT116 cells (Pelish et al., 2015), proliferation is not affected. This eliminated potential confounding effects, such as induction of cell cycle arrest or death, which could have complicated our analyses. Second, CDK8 is a colon cancer oncogene that was uncovered, in part, by an shRNA screen in HCT116 cells (Firestein et al., 2008). Third, published gene expression data exist in HCT116 cells with stable CDK8 or CDK19 knockdown (Donner et al., 2010; Galbraith et al., 2013), which allowed us to directly compare and de-couple the effects of subunit knockdown vs. targeted inhibition of kinase activity.

RESULTS

Quantitative phosphoproteomics in HCT116 cells ± CA

To identify cellular CDK8 and CDK19 substrates, we used stable isotope labeling of amino acids in cell culture (SILAC) coupled with a phosphoproteomics workflow. Experiments were completed in HCT116 cells supplemented with heavy (Arg10, Lys8) or light (Arg0, Lys0) amino acids. Control (DMSO) and CA-treated cells were harvested and mixed 1:1 based on total protein content (CA structure shown in **Fig. 1A**). Phosphopeptides were isolated using titanium enrichment, followed by offline electrostatic repulsion hydrophilic interaction chromatography (ERLIC) with LC-MS/MS for phosphosite identification (**Fig. 1B**). We collected 24 fractions during ERLIC fractionation, with an average phosphopeptide enrichment of over 50% in biological triplicate experiments (**Fig. 1C**). In total, over 16,000 heavy-light (H/L) phosphosite ratios were quantified (**Table S1**) and over 12,000 were present in at least two biological replicates (**Fig. 1D**).

The majority of phosphosites were unaffected by CA treatment, clustering around zero in a $\log_2$ plot of H/L SILAC ratios across replicate experiments (**Fig. 1D**). This result indicated good reproducibility and provided further validation of CA specificity. Many decreased phosphosites were highly correlated across replicates (highlighted green in **Fig. 1D**); in addition, we identified a smaller number of phosphosites that increased upon CA treatment (highlighted peach in **Fig. 1D**; **Table S2**). Representative mass spectra for SILAC pairs shown in **Figure 1E** and **1F** are from experiments in which either light (**E**) or heavy (**F**) cells were treated with CA. For two of three replicates, the heavy population of cells was CA treated, whereas in one replicate light cells were CA treated, representing a label swap. For data analysis purposes, a reciprocal of the H/L ratio was calculated for the label swap experiment, such that decreased H/L ratios could be evaluated across all biological replicates.

Mediator kinase substrates are largely transcription-associated proteins

The phosphoproteomics workflow in **Fig. 1B** identified novel phosphosites whose intensities decreased significantly with CA treatment (**Fig. 2A**). We identified 78 phosphosites, represented in 64 proteins, that we designated as high confidence based upon 1) their quantification in at least two of three biological replicates, 2) a reproducible mean H/L ratio across replicates, and 3) a significant decrease in H/L ratio with CA treatment as determined by an empirical Bayes analysis (Margolin et al., 2009; Ritchie et al., 2015). These high-confidence phosphosites are summarized in **Table 1** and **Figure 2A**, and all quantified phosphosites are shown in **Table S1**. To ensure that a reduced H/L ratio did not result simply from a change in protein level, we completed a quantitative proteome analysis in parallel with phosphoproteomics. Importantly, very few high confidence phosphosites exhibited any change at the protein level with one hour of CA treatment (**Table S2**). Those that did change somewhat were FOXC1, MAML1, KDM3A, and ATF2, although some of these changes were not consistent across deep proteome replicates, and most of the phosphosite changes remained significant even after accounting for small changes in protein level. Although phosphosites not designated as high confidence sites could represent bona-fide Mediator kinase substrates (e.g. those that are quantified in only one biological replicate) we will only discuss targets designated as high confidence based on the criteria above.

To determine whether a H/L ratio for a phosphosite changed significantly with CA treatment across replicates, we employed an empirical Bayes statistical approach using the *limma* software package (Ritchie et al., 2015). An empirical Bayesian framework allowed for the calculation of adjusted p-values for each phosphosite (**Fig. 2B**). This approach can account for experiment-specific differences, which is advantageous compared to more arbitrary approaches, such as a universal fold-change cutoff (Margolin et al., 2009). We found that more phosphosite ratios decreased than increased upon CA treatment, as expected with targeted kinase inhibition for a short amount of time. This is shown by a higher number of data points on the left side of the volcano plot compared to the right side, using an adjusted p-value cutoff of 0.1 (**Fig. 2B**; see also **Supplemental Note**).

We used iceLOGO (Colaert et al., 2009) to determine statistically enriched motifs within the identified Mediator kinase substrates. We found that the majority of the phosphosites

contained an S/T-P motif (**Fig. S1A**). Additionally, a proline at the −2 and −1 positions relative to the phosphorylation site was overrepresented. These data support the notion that many CDK8 phosphorylation sites occur within PX(S/T)P motifs as previously suggested (Alarcon et al., 2009; Bancerek et al., 2013). Serine was more frequently phosphorylated than threonine (**Fig. S1A**) and we did not see evidence for overrepresentation of basic residues at positions C-terminal to the phosphosite, as observed with other CDK motifs (Ubersax and Ferrell, 2007).

Because few substrates for human CDK8/19 have been identified, the analysis uncovered many phosphosite targets (**Table 1)**. Many targets are DNA-binding transcription factors (TFs), chromatin regulators, or other known regulators of pol II activity (**Fig. 2A**, **Fig. S1B**), consistent with the established role of CDK8 in transcription. Additional substrates, including proteins implicated in DNA replication and repair (BRCA1, MDC1) and ubiquitination (HUWE1, CUL4B) suggest biological roles for Mediator kinases beyond transcription. A known CDK8 substrate, STAT1 S727 (Bancerek et al., 2013), was identified as a high confidence target, and other novel phosphosites reside in proteins that interact with CDK8-Mediator and/or the CDK8 module, including AFF4, MAML1, and Mediator subunits (**Fig. 2A**, **Table 1**). AFF4 is a core component of the super-elongation complex (SEC; (Luo et al., 2012)), which co-purifies with CDK8-Mediator (Ebmeier and Taatjes, 2010), and MAML1 is a Notch pathway co-activator that recruits CDK8 to Notch-dependent genes where it phosphorylates the Notch ICD (Fryer et al., 2004).

We submitted the 64 CDK8/19 substrate proteins to the STRING protein-protein interaction database (Szklarczyk et al., 2015) and found that six Mediator complex subunits, three subunits of the TIP60/NuA4 complex (EPC2, DMAP1, MRGBP), and two subunits of the NuRD complex (CHD3 and CHD4) were represented (high confidence score, ≥ 0.7; **Fig. S1C**). The TIP60/NuA4 and NuRD complexes are multi-subunit assemblies that possess multiple enzymatic activities, including nucleosome remodeling, acetyltransferase, and deacetylase activities. Additionally, this analysis identified a network of interacting proteins involved in DNA damage repair (**Fig. S1C**), as well as an interaction between XRN2 and SETX. Taken together, these data suggest that Mediator kinases regulate multiple and diverse cellular processes, potentially via several distinct multi-subunit assemblies.

Validation of selected Mediator kinase substrates

To further validate the CDK8/19 substrates identified with SILAC-based phosphoproteomics, we performed *in vitro* kinase assays, western blots, and MS experiments. We selected proteins representing different classes of substrates (**Fig. 2A**) for further evaluation. The DNA-binding TF STAT1, a previously identified CDK8 kinase substrate (Bancerek et al., 2013), was probed by western blot in IFN-γ induced HCT116 cells (**Fig. 3A**). This experiment confirmed STAT1 S727 as a Mediator kinase substrate in HCT116 cells, and also showed CA-dependent inhibition at low nM concentrations, as reported previously (Pelish et al., 2015).

Among the chromatin modification and regulation substrates, we examined SIRT1, in part because an antibody against the phosphorylated SIRT1 T530 site was commercially available. When HCT116 cells were treated with CA, we noted a decrease in SIRT1 T530

phosphorylation (**Fig. 3B** and **3C**). Total SIRT1 levels were unaffected by CA treatment, and levels of the CDK8 module subunits CDK8, CCNC, and MED12 were not changed by treatment with the compound (**Fig. 3B**). The approximately 50% reduction in phospho-SIRT1 did not change with increasing CA concentration, indicative of CA selectivity (Pelish et al., 2015). Although other kinases, such as CDK1 and JNK, are known to phosphorylate this site (Sasaki et al., 2008), treatment with inhibitors of CDK1 (RO-3306) and JNK family kinases (SP600125) did not seem to impact SIRT1 T530 phosphorylation; in fact, we were unable to completely reduce SIRT1 phospho-T530 detection, even when treating with all three inhibitors (**Fig. S2**). *In vitro* kinase assays with purified CDK8 module and SIRT1 confirmed CDK8-dependent SIRT1 T530 phosphorylation by western blot (**Fig. 3D**).

We next tested two different substrates, RIF1 and TP53BP1, linked to DNA replication and repair. Because these proteins are very large (each over 200 kDa), we expressed GST-tagged fragments (ca. 100 residues) surrounding the phosphosite. As shown in **Figure 3E**, the CDK8 module phosphorylated these substrates, whereas point mutations (S to A) at the identified phosphorylation site(s) greatly reduced substrate phosphorylation, supporting these sites as CDK8 module targets *in vitro* (**Fig. 3E**).

We also confirmed phosphorylation sites in MED12 and MED13 using *in vitro* kinase assays using the recombinant CDK8 module (containing CDK8, CCNC MED12, MED13) purified from insect cells. Incubation of the CDK8 module with ATP and subsequent TiO_2 enrichment and MS analysis confirmed both S688 on MED12 and S749 on MED13 as substrates (**Fig. 3F** and **3G**). We did not identify the CCNC site from these experiments because the site identified from CA-treated HCT116 cells is not present in the canonical CCNC isoform used for recombinant CDK8 module expression and purification.

The data summarized in **Figure 3** verified each of seven high-confidence Mediator kinase sites, representing about 10% of all high-confidence sites listed in **Table 1**. These results, combined with previous data demonstrating CA potency and specificity (Pelish et al., 2015), support the substrates listed in **Table 1** as Mediator kinase targets. Although extensive kinome profiling has demonstrated CA specificity, we conducted *in vitro* kinase assays using a shared substrate, the pol II CTD, and found that CDK1, ERK2, and GSK3β activity was unaffected by CA treatment, even at concentrations ten-fold above those used for proteomic and gene expression analyses (**Fig. 3H**).

Mediator kinase inhibition has limited and specialized effects on transcription

As Mediator-associated kinases, it was plausible that inhibition of CDK8 and CDK19 activity could affect expression of large numbers of genes. We analyzed gene expression (RNA-Seq) data from CA treated HCT116 cells (**Table S3**). To minimize secondary or indirect effects resulting from long-term Mediator kinase inhibition, we completed RNA-Seq after a three-hour CA treatment (100 nM); this also helped match mRNA changes with measured phosphorylation changes that were determined after one-hour CA treatment. RNA-Seq analysis identified 150 genes whose expression changed significantly with CA treatment (**Fig. 4A**). Among these genes, the magnitude of change in expression was modest (largely 1.2 – 2 fold), indicating that CDK8/19 activity *per se* is not a major driver of their

transcription, at least in the context of this analysis (HCT116 cells under normal growth conditions). Such modest gene expression changes were also observed in CA-sensitive cell lines (e.g. MOLM-14), although the genes affected were distinct (Pelish et al., 2015).

Gene expression changes in CA-treated cells compared to CDK8 or CDK19 knockdown

Because CA inhibits both CDK8 and CDK19 kinases, we used previously published HCT116 microarray datasets (normal growth conditions), in which either CDK8 or CDK19 had been stably knocked down (Donner et al., 2010; Galbraith et al., 2013), as a comparison to CA-treated HCT116 cells. Only genes exhibiting 1.5-fold change in expression or greater, with p-values <0.05, were used from the microarray data; these genes were compared to our RNA-seq analysis in which cells were treated with 100 nM CA for three hours. We observed only a modest overlap among genes differentially expressed (**Fig. 4B**; note that because CA inhibits both CDK8 and CDK19, gene sets for CDK8 or CDK19 knockdown were combined). Because cellular knockdown experiments take over 24 hours to manifest, the modest correlation in gene expression changes could reflect the short time of CA treatment. However, RNA-seq analyses after 24 hour CA treatment revealed similarly low numbers of shared gene expression changes (**Fig. 4C**). These results, further summarized in **Figure S3**, suggest that the physical presence of the CDK8 or CDK19 protein has distinct effects on transcription compared to targeted kinase inhibition.

Functional links between gene expression changes and Mediator kinase substrates

Because many Mediator kinase substrates are transcription factors (**Fig. 2A**), we hypothesized that some of the observed differences in gene expression due to CDK8/19 inhibition might be caused by changes in TF function. To begin to address this hypothesis, we extracted promoter sequences (± 2kb from TSS) for genes that were differentially expressed (increased or decreased expression) 3h CA treatment. F-Match was then used to compare promoter sequences to controls to determine if any TF binding sites, reported as Transfac matrices, were over-represented. The ratio of this increase (CA-treated cells vs. DMSO controls) is displayed for over-represented sites in **Figure 4D**. We found that many of the identified Transfac matrices for genes whose expression increased or decreased with CA treatment were mutually exclusive (**Fig. 4D**). That is, an enriched TF binding site in CA increased genes was generally not present in CA decreased genes, and vice versa. A hypergeometric test confirmed a significant overlap (p-value = $1.15E^{-5}$) between Mediator kinase targets identified in **Table 1** and Transfac matrices identified in our gene expression promoter analysis (**Fig. S3F**).

Many of the Transfac matrices identified by F-match (**Fig. 4D**) can be traced back to Mediator kinase activity, as summarized in **Figure S4**. For example, the RREB1 TF was identified in both the F-match analysis (RREB1_01) and the SILAC phosphoproteomics (**Table 1**). Enriched TF binding sites were observed for genes with altered expression in CA-treated HCT116 cells (**Fig. 4A**), including MYC, a β-catenin target gene, EGR1 (i.e. KROX_Q6), and HES1, a Notch pathway target gene. Moreover, the MGA and NAB2 proteins, each high-confidence Mediator kinase substrates, are known regulators of MYC and EGR1 activity, respectively (Hurlin et al., 1999; Svaren et al., 1996). Transfac matrices representing the AP2 and ATF family of TFs (e.g. AP2alpha_01, ATF1_Q6) were also

uncovered in the F-match analysis. The Mediator kinase target KLF12 is a well-established repressor of AP2α activity (gene name: TFAP2A) (Imhof et al., 1999), whereas the ATF2 and ATF7 proteins were each identified as Mediator kinase targets. Finally, enriched binding sites for E2F1 and SREBP, previously identified CDK8 kinase substrates (Morris et al., 2008; Zhao et al., 2012), were found by the F-match analysis shown in **Figure 4D**. Although these TFs were not identified in our HCT116 phosphoproteomics experiments, several co-regulators of E2F1 or SREBP activity (e.g. MGA, SIRT1; see Discussion) were among the high-confidence substrates listed in **Table 1**. Thus, there are many functional links between CA-dependent changes in gene expression (**Fig. 4A**) and the Mediator kinase targets shown in **Table 1**.

Cellular proteome changes resulting from Mediator kinase inhibition

The ability of CDK8-dependent phosphorylation to regulate protein turnover has been reported in both yeast and human cells (Alarcon et al., 2009; Fryer et al., 2004; Nelson et al., 2003; Raithatha et al., 2012). We therefore hypothesized that CDK8/19 activity might modulate protein abundance for some of the substrates identified here. Rather than focus on selected Mediator kinase targets, we performed quantitative proteome analyses in CA-treated cells vs. DMSO controls at six time points (t = 0h, 1h, 3h, 6h, 18h, and 24h). In this way, we were able to interrogate many cellular proteins at once, and correlate changes in Mediator kinase activity with increased or decreased protein abundance. To complete these analyses, we used SILAC labeled HCT116 cells, consistent with the phosphoproteomics experiments.

The analysis consisted of a CA treatment time course from 0 to 24 hours, with six time points being used in total to treat heavy (Arg10, Lys8) or light (Arg0, Lys0) HCT116 cell populations in biological replicate experiments (**Fig. 5A, B**). Peptides were harvested in a manner similar to that used for phosphoproteomics, and 17 fractions from basic reversed-phase chromatography were analyzed for changes in H/L ratio at each time point. We found a high number of overlapping proteins across replicates, and CA treatment did not affect global H/L ratios for proteins across the time course in the replicates (**Fig. 5B**). Given the ability of CDK8 to promote substrate turnover in response to specific biological phenomena (e.g. starvation) (Nelson et al., 2003; Raithatha et al., 2012), we were somewhat surprised to find that CDK8/19 inhibition did not notably alter the abundance of the target proteins listed in **Table 1**, with the exception of MED13 and MED13L. A list of all quantified proteins in CA-treated vs. untreated cells (0 – 24h) is provided in **Table S4**.

An empirical Bayes analysis of the data suggested that most proteome changes occurred at either 18 or 24 hours when compared to control (0 hr, in which both populations were DMSO treated), as shown by the volcano plot in **Fig. 5C**. Approximately 200 proteins showed significant changes in abundance and these are listed in **Table S5** (adj. pval < 0.1). To further examine changes in the proteome with CA treatment, gene set enrichment analysis (GSEA) was employed (Subramanian et al., 2005). Using the hallmark gene set collection, we identified biological processes that displayed significant enrichment scores and false discovery rates (**Fig. 5D** and **Table S6**). Of these signatures, several have been previously shown to be regulated by CDK8, including Wnt/β-catenin signaling, Notch

signaling, hypoxia, interferon gamma response, and KRAS signaling (Bancerek et al., 2013; Firestein et al., 2008; Fryer et al., 2004; Galbraith et al., 2013; Morris et al., 2008; Xu et al., 2015). CDK8-dependent transcriptional changes have been implicated in regulation of these pathways and therefore, the proteome data corroborate these findings at the protein level. The GSEA results also reveal that proteome changes may selectively affect metabolic pathways in CA-treated HCT116 cells, with several (e.g. cholesterol homeostasis, fatty acid metabolism) previously linked to CDK8 kinase activity in model organisms (Zhao et al., 2012).

DISCUSSION

The natural product cortistatin A (CA) is an exceptionally selective inhibitor of the Mediator kinases CDK8 and CDK19 (Pelish et al., 2015). As such, it provided a means to rapidly and selectively probe CDK8 and CDK19-dependent phosphoproteome changes in human cells. Because of their association with Mediator, CDK8 and CDK19 were expected to phosphorylate proteins involved in regulating pol II activity and chromatin architecture. In accordance with these expectations, our data support a primary role for Mediator kinases in pol II transcription and chromatin regulation. Strikingly, however, the direct impact of Mediator kinase inhibition on global pol II transcription was modest and affected a limited set of genes, at least under the conditions of this study. Limited transcriptional effects were also observed in CA-sensitive AML cell lines (Pelish et al., 2015).

At the gene expression level, it appears that Mediator kinases predominantly “regulate the regulators” of transcription. Many genes whose expression increased or decreased 1.5-fold or greater upon CA treatment are DNA-binding TFs or general transcription or chromatin regulators. Similarly, DNA-binding TFs and pol II transcription or chromatin regulators represented the majority of high-confidence CDK8/CDK19 kinase targets from the SILAC phosphoproteomics experiments. Quantitative proteomic data across a 24-hour time course implicated numerous signaling and metabolic pathways that appear to be regulated by Mediator kinase activity under normal growth conditions. Whereas these pathways can be linked to known transcriptional or phosphorylation targets of CDK8/CDK19 or those now identified here, much additional investigation will be required to delineate the molecular mechanisms by which Mediator kinases regulate specific signaling pathways or transcriptional processes.

CDK8/19 phosphorylate Mediator subunits and post-initiation transcription regulators

CDK8 can reversibly associate with Mediator to form a CDK8-Mediator complex (Taatjes et al., 2002), and immunoprecipitation-mass spectrometry experiments in HeLa or HEK293T cells suggest CDK19 interacts similarly with Mediator (Daniels et al., 2013; Ebmeier and Taatjes, 2010; Sato et al., 2004). We identified eight high-confidence CDK8/19 phosphorylation sites in six different Mediator subunits: CCNC, MED12, MED13, MED13L, MED14, and MED26. CCNC, MED12, MED13, and MED13L each associate with CDK8 or CDK19 as part of the kinase module of Mediator. MED13 appears to be important for physical interaction between the kinase module and Mediator (Knuesel et al., 2009), and previous studies have shown that increased MED13 or MED13L abundance can

increase the proportion of CDK8-Mediator vs. core Mediator in cells (Davis et al., 2013). These previous results were shown in the context of inhibition of the E3 ubiquitin ligase FBW7, which ubiquitylates MED13 and MED13L to promote their degradation. Our quantitative whole proteome data showed that the abundance of MED13 and MED13L were each increased in CA-treated HCT116 cells. FBW7-dependent ubiquitylation of MED13 or MED13L required prior modification at residue T326, a phospho-degron site in MED13 and MED13L (Davis et al., 2013). The CDK8/19 sites identified in MED13 and MED13L are distinct (residue S749 and residue S878, respectively) and do not overlap with known or predicted phospho-degron motifs; thus, it remains unclear how Mediator kinase activity may affect MED13 or MED13L protein levels.

The MED26 subunit is generally absent from CDK8-Mediator purifications (Ebmeier and Taatjes, 2010; Sato et al., 2004; Taatjes et al., 2002) and hence, its phosphorylation by CDK8 or CDK19 may promote MED26 dissociation from Mediator. The CDK8/19 modification site on MED26 (S314), however, does not reside in regions required for Mediator association (Takahashi et al., 2011). The MED14 subunit is an important architectural factor within Mediator, and structural studies with reconstituted partial complexes and crosslinking-mass spectrometry (CXMS) revealed MED14 crosslinks with several Mediator subunits, including MED8 and MED7, involving MED14 residues 1256 and 1295, respectively (Cevher et al., 2014). These reside some distance (in sequence space) from the Mediator kinase phosphorylation sites (S1112, S1128, S1136). Furthermore, CXMS and cryo-EM data with reconstituted yeast Mediator and yeast pol II revealed MED14 interactions with pol II and TFIIF (Plaschka et al., 2015). However, the *S. cerevisiae* Med14 subunit from this study consisted of residues 1-755 (of 1082 residues in yeast Med14) and the human MED14 S1112, S1128, and S1136 residues do not appear to be conserved.

Knockdown experiments have implicated the CDK8 protein in the regulation of transcription elongation and/or pol II pausing or pause release (Donner et al., 2010; Galbraith et al., 2013). Furthermore, ChIP-Seq data from CA-treated MOLM-14 cells indicated a reduced pol II travel ratio (TR; ratio of promoter-bound pol II vs. pol II in gene body) at genes whose expression was up-regulated by CA (Pelish et al., 2015), implicating Mediator kinase activity in pol II pausing or pause release. The reduced TR in CA-treated cells could also reflect inhibition of premature pol II termination. Here, we identified AFF4, NELFA, MED26, POLR2M, SETX, and XRN2 as high-confidence Mediator kinase targets, and each of these factors has been implicated in regulation of pol II pausing, premature termination, or elongation (Brannan et al., 2012; Cheng et al., 2012; Jishage et al., 2012; Kwak and Lis, 2013; Lin et al., 2010; Takahashi et al., 2011; Wagschal et al., 2012).

Mediator kinases as potential metabolic regulators

CDK8 orthologs in *Drosophila* and yeast have been linked to lipid and glucose metabolism and regulation of cellular responses to nutrient stress (Kuchin et al., 1995; Lindsay et al., 2014; Mousley et al., 2012; Zhao et al., 2012). Upon Mediator kinase inhibition by CA, we observed changes in the abundance of about 200 proteins (**Fig. 5**), including many involved in basic metabolic pathways such as oxidative phosphorylation, fatty acid metabolism, and

cholesterol homeostasis. MED13 and CCNC appear to regulate mitochondrial function in yeast (Cooper et al., 2014; Khakhina et al., 2014), and over-expression of MED13 in mouse cardiac tissue alters fatty acid metabolism, β-oxidation, and mitochondrial content (Baskin et al., 2014). We identified MED13 and CCNC as Mediator kinase substrates and observed an increase in MED13 protein levels upon CA treatment, which could contribute to altered fatty acid metabolism or oxidative phosphorylation observed in CA-treated cells (**Fig. 5D**).

CDK8 kinase activity has previously been linked to cholesterol metabolism and fatty acid synthesis via regulation of SREBP. In particular, CDK8-dependent phosphorylation of SREBP residue T402 correlated with SREBP degradation in *Drosophila* and mouse cells (Zhao et al., 2012). GSEA analysis of whole proteome data identified changes in the cholesterol homeostasis, adipogenesis, and fatty acid metabolism hallmark signatures in CA-treated cells (**Fig. 5D**). Moreover, F-match identified SREBP binding motifs as over-represented among genes whose expression changed upon CA treatment (**Fig. 4D**). Whereas phosphorylation of SREBP T402 was detected in our phosphoproteomics experiments, its level was not altered in CA-treated cells, suggesting alternate means of Mediator kinase-dependent SREBP regulation in HCT116 cells. Other kinases, including GSK3 (Sundqvist et al., 2005), are known to target SREBP T402 and we have confirmed that CA does not inhibit GSK3β in cell lysates (Pelish et al., 2015) or in *in vitro* kinase assays with the purified protein (**Fig. 3H**). Therefore, the SREBP T402 phosphorylation level may remain constant in CA-treated cells due to other kinases targeting this site. Alternately, SREBP may not be a substrate for CDK8 in HCT116 cells. SIRT1, a validated Mediator kinase target, can negatively regulate SREBP activity through deacetylation (Walker et al., 2010). The Mediator kinases phosphorylate SIRT1 at residue T530, and phosphorylation at T530 has been shown to activate the SIRT1 deacetylase (Sasaki et al., 2008). Thus, via SIRT1 and potentially other substrates, Mediator kinases may regulate cholesterol or fatty acid metabolism independent of direct SREBP phosphorylation in HCT116 cells.

Human Mediator kinases and TF turnover

Previous studies revealed that phosphorylation of nutrient-responsive TFs Gcn4, Ste12, or Phd1 by yeast Cdk8 promoted their degradation (Chi et al., 2001; Nelson et al., 2003; Raithatha et al., 2012). Studies in metazoans have shown evidence for CDK8-dependent phosphorylation of the TFs SMAD1, SMAD3, Notch ICD, SREBP, E2F1, and STAT1 (Alarcon et al., 2009; Bancerek et al., 2013; Fryer et al., 2004; Morris et al., 2008; Zhao et al., 2012). Among these, increased degradation of the Notch ICD, SMAD1, SMAD3, and SREBP correlated with phosphorylation. For these reasons, we anticipated that inhibition of CDK8 and CDK19 kinase activity would affect the protein levels of a subset of their targets. Whole proteome data revealed no evidence that TF phosphorylation by Mediator kinases affected their stability, even with analyses at 1, 3, 6, 18, or 24 hours of CA treatment. In fact, we found little evidence for altered stability of any high-confidence Mediator kinase targets, with the notable exception of MED13 and MED13L. Despite this result, cell type or context may be key factors that dictate the effect of Mediator kinase phosphorylation on protein turnover. Here, we evaluated HCT116 cells in normal growth conditions whereas Mediator kinases may in fact more generally regulate substrate protein turnover during stress responses or at different developmental stages.

Whereas no changes in TF turnover were evident from the whole proteome data in CA-treated vs. control cells, we identified many links between the gene expression changes and the phosphoproteomics data (**Fig. S4**). These results are consistent with Mediator kinases affecting TF activity in HCT116 cells under normal growth conditions, rather than TF turnover.

CDK8 as a colon cancer oncogene: Mediator kinase inhibition vs. subunit knockdown

CDK8 was identified as a colon cancer oncogene in part through an shRNA screen for genes required for HCT116 cell proliferation (Firestein et al., 2008). CDK8 was one of 166 candidates in this screen; CDK8 was also identified in a screen for factors required for activation of a β-catenin-driven reporter in a different colon cancer line, DLD-1 (Firestein et al., 2008). Our analyses with CA indicate that, in contrast to CDK8 knockdown, Mediator kinase inhibition does not affect HCT116 cell growth (Pelish et al., 2015). These findings highlight the distinction between physical loss of a protein vs. targeted inhibition of its enzymatic activity.

As a TF, β-catenin assembles with the DNA-binding proteins TCF and LEF-1 to activate genes that drive cell proliferation. HCT116 cells are heterozygous for a mutant β-catenin protein that is resistant to degradation (Morin et al., 1997). Consequently, HCT116 cells have increased β-catenin levels and are considered “β-catenin-dependent”. Consistent with an oncogenic function for CDK8, CDK8 knockdown prevented activation of β-catenin target genes in colon cancer cell lines (Firestein et al., 2008). In addition, the E2F1 TF has been shown to be an important negative regulator of β-catenin stability (through unknown mechanisms), and elevated levels of the CDK8 protein, as observed in HCT116 cells (Firestein et al., 2008), can block E2F1-dependent inhibition of β-catenin target gene expression (Morris et al., 2008). Thus, in colon cancer cells, the CDK8 protein appears to up-regulate β-catenin target gene expression in two ways: as a β-catenin co-activator and as an inhibitor of E2F1 activity.

Whereas E2F1 and β-catenin activity or stability is known to be regulated by phosphorylation, we did not observe significant changes in E2F1 or β-catenin protein or phosphopeptide levels in CA-treated HCT116 cells. An F-match analysis based upon gene expression changes in CA-treated cells, however, identified E2F binding motifs as over-represented (**Fig. 4D**), and Ingenuity Pathway Analysis (IPA) of upstream regulators identified β-catenin target genes as over-represented among those whose expression increased or decreased upon CA treatment (**Table S7**). GSEA of our proteomics data (CA-treated vs. untreated, 0 – 24h) revealed up-regulation of both the E2F1 and β-catenin pathways (**Fig. 5D**). Furthermore, numerous high-confidence Mediator kinase substrates are known to directly regulate β-catenin or E2F activity, and these are summarized in **Table S8**.

Although these results implicate Mediator kinase activity in the regulation of E2F1 and β-catenin transcription networks in HCT116 cells, the effects of Mediator kinase inhibition are clearly distinct from CDK8 or CDK19 knockdown (Donner et al., 2010; Firestein et al., 2008; Galbraith et al., 2013). This was not unexpected, as the physical presence of an enzyme typically serves structural roles, such as maintaining the integrity of a multi-protein complex. For example, ablation of the CDK7 ortholog in yeast (Kin28) abolishes essentially

all pol II transcription (Holstege et al., 1998), in contrast to targeted inhibition of Kin28 activity (Kanin et al., 2007). Direct comparison of the transcriptional changes resulting from physical loss of the CDK8 or CDK19 protein versus targeted inhibition of kinase activity (i.e. with protein levels remaining intact) revealed stark differences in both the genes affected and in the magnitude of gene expression changes. These differences highlight the importance of a structural or "scaffolding" role of the CDK8 or CDK19 proteins. Indeed, CDK8 knockdown decreases MED12 levels and increases CDK19 protein levels in HCT116 cells (Donner et al., 2010; Galbraith et al., 2013), which likely contributes to the distinct gene expression and anti-proliferative effects of CDK8 knockdown (Firestein et al., 2008) compared with kinase inhibition by CA. Because CA inhibits CDK19 as well as CDK8 (Pelish et al., 2015), this may also result in compensatory effects that distinguish the CDK8 knockdown phenotype from CDK8/CDK19 inhibition. Future studies are needed to more precisely establish the roles of CDK8 vs. CDK19 in regulating the elaborate E2F1, β-catenin, and other inter-related signaling networks that contribute to HCT116 survival and proliferation.

Concluding remarks

This study provides a large-scale identification of Mediator kinase substrates and the impact of Mediator kinase activity on pol II transcription and the cellular proteome. In comparison with the ~170 potential CDK9 kinase substrates recently identified in HCT116 cells (Sanso et al., 2016), it is notable that the high-confidence substrates for CDK9 are distinct from the Mediator kinases. This further suggests that CDK9 (e.g. as part of P-TEFb or the SEC) and Mediator kinases play non-redundant roles in transcription regulation.

Our results were enabled by the rigorous biochemical, cellular, and biophysical characterization of CA, which demonstrated that it represents an unusual case of an inhibitor that is truly selective for Mediator kinases in human cells (Pelish et al., 2015). The data and methodologies presented provide a valuable resource for further delineation of the molecular mechanisms whereby Mediator kinases, and their substrates, regulate processes that are fundamentally important in human development and disease. For example, the methodologies described could be applied toward other cell types or contexts to uncover cell type- or context-specific roles for Mediator kinases. Alternately, the Mediator kinase targets or proteome changes identified here could be further tested for their mechanistic role(s) in regulating chromatin structure and function, DNA repair or replication, cell metabolism, or pol II transcription.

EXPERIMENTAL PROCEDURES

Cell culture

HCT116 cells were cultured in DMEM supplemented with 10% FBS and penicillin/streptomycin. Cells were maintained at 37°C and 5% CO_2.

SILAC labeling

HCT116 cells were cultured in DMEM lacking arginine and lysine (Pierce-88420) supplemented with either Arg10 (33.6 μg/ml) and Lys8 (73 μg/ml) or Arg0 and Lys0 for

heavy and light treatment, respectively. After six passages at 1:3 ratio, cells were tested for Arg/Lys incorporation and were subsequently supplemented with 200mg/L of proline (Sigma-P5607) as a small amount of Arg→Pro conversion was detected. Cells were maintained in 10% dialyzed FBS and penicillin/streptomycin.

TiO_2 phosphopeptide enrichment, ERLIC chromatography, and LC/MS/MS

Protocols were carried out as described (Stuart et al., 2015). An Orbitrap LTQ (Thermo Fisher) was used for phosphoproteomics, and an Orbitrap Velos (Thermo Fisher) was used for quantitative proteome analysis.

In vitro kinase assays

Assays were done essentially as described (Bancerek et al., 2013). Additional details provided in Supplemental Experimental Procedures.

Gene expression comparison between CA treated HCT116 cells and shRNA CDK8/19

shRNA CDK8 and CDK19 microarray data were obtained from the GEO (accession GSE38061) and data under the “normoxia” tab were used for the comparison to CA treated cells.

Supplementary Material

Refer to Web version on PubMed Central for supplementary material.

ACKNOWLEDGMENTS

Z.C.P. would like to thank P. Kovarik for STAT1 antibodies, J. Liddle and S. Stuart for assistance and phospho-ERK, and C. Poss and R. Burgundy for useful discussions. We thank J. Balsbaugh at the Mass Spectrometry and Proteomics core facility at UC-Boulder. Expression of CDK8 module was completed at the Tissue Culture Shared Resource at the UC Cancer Center, supported by P30-CA046934. RNA-seq was carried out at the Genomics Shared Resource at the UC Cancer Center, supported by P30-CA046934. This work was supported by R01 CA170741 (DJT), R21 CA175448 (DJT and WMO), F31 CA180419 (ZCP) and T32 GM08759 (ZCP).

REFERENCES

Alarcon C, Zaromytidou A, Xi Q, Gao S, Yu J, Fujisawa S, Barlas A, Miller AN, Manova-Todorova K, Macias MJ, et al. Nuclear CDKs drive Smad transcriptional activation and turnover in BMP and TGF-b pathways. Cell. 2009; 139:757–769. [PubMed: 19914168]

Allen BL, Taatjes DJ. The Mediator complex: a central integrator of transcription. Nat Rev Mol Cell Biol. 2015; 16:155–166. [PubMed: 25693131]

Bancerek J, Poss ZC, Steinparzer I, Sedlyarov V, Pfaffenwimmer T, Mikulic I, Dolken L, Strobl B, Muller M, Taatjes DJ, et al. CDK8 Kinase Phosphorylates Transcription Factor STAT1 to Selectively Regulate the Interferon Response. Immunity. 2013; 38:250–262. [PubMed: 23352233]

Baskin KK, Grueter CE, Kusminski CM, Holland WL, Bookout AL, Satapati S, Kong YM, Burgess SC, Malloy CR, Scherer PE, et al. MED13-dependent signaling from the heart confers leanness by enhancing metabolism in adipose tissue and liver. EMBO Mol Med. 2014; 6:1610–1621. [PubMed: 25422356]

Brannan K, Kim H, Erickson B, Glover-Cutter K, Kim S, Fong N, Kiemele L, Hansen K, Davis R, Lykke-Andersen J, et al. mRNA decapping factors and the exonuclease Xrn2 function in widespread premature termination of RNA polymerase II transcription. Mol Cell. 2012; 46:311–324. [PubMed: 22483619]

Cevher MA, Shi Y, Li D, Chait BT, Malik S, Roeder RG. Reconstitution of active human core Mediator complex reveals a critical role of the MED14 subunit. Nat Struct Mol Biol. 2014; 21:1028–1034. [PubMed: 25383669]

Cheng B, Li T, Rahl PB, Adamson TE, Loudas NB, Guo J, Varzavand K, Cooper JJ, Hu X, Gnatt A, et al. Functional association of Gdown1 with RNA polymerase II poised on human genes. Mol Cell. 2012; 45:38–50. [PubMed: 22244331]

Chi Y, Huddleston MJ, Zhang X, Young RA, Annan RS, Carr SA, Deshaies RA. Negative regulation of Gcn4 and Msn2 transcription factors by Srb10 cyclin-dependent kinase. Genes Dev. 2001; 15:1078–1092. [PubMed: 11331604]

Colaert N, Helsens K, Martens L, Vandekerckhove J, Gevaert K. Improved visualization of protein consensus sequences by iceLogo. Nat Methods. 2009; 6:786–787. [PubMed: 19876014]

Cooper KF, Khakhina S, Kim SK, Strich R. Stress-induced nuclear-to-cytoplasmic translocation of cyclin C promotes mitochondrial fission in yeast. Dev Cell. 2014; 28:161–173. [PubMed: 24439911]

Daniels DL, Ford M, Schwinn MK, Benink H, Galbraith MD, Amunugama R, Jones R, Allen D, Okazaki N, Yamakawa H, et al. Mutual exclusivity of MED12/MED12L, MED13/13L, and CDK8/19 paralogs revealed within the CDK-Mediator kinase module. J Proteomics Bioinform. 2013; S2:004.

Davis MA, Larimore EA, Fissel BM, Swanger J, Taatjes DJ, Clurman BE. The SCF Fbw7 ubiquitin ligase degrades MED13 and MED13L and regulates CDK8 module association with Mediator. Genes Dev. 2013; 27:151–156. [PubMed: 23322298]

Donner AJ, Ebmeier CC, Taatjes DJ, Espinosa JM. CDK8 is a positive regulator of transcriptional elongation within the serum response network. Nat Struct Mol Biol. 2010; 17:194–201. [PubMed: 20098423]

Ebmeier CC, Taatjes DJ. Activator-Mediator binding regulates Mediator-cofactor interactions. Proc Natl Acad Sci U S A. 2010; 107:11283–11288. [PubMed: 20534441]

Firestein R, Bass AJ, Kim SY, Dunn IF, Silver SJ, Guney I, Freed E, Ligon AH, Vena N, Ogino S, et al. CDK8 is a colorectal cancer oncogene that regulates b-catenin activity. Nature. 2008; 455:547–551. [PubMed: 18794900]

Fryer CJ, White JB, Jones KA. Mastermind recruits CycC:Cdk8 to phosphorylate the notch ICD and coordinate activation with turnover. Mol Cell. 2004; 16:509–520. [PubMed: 15546612]

Galbraith MD, Allen MA, Bensard CL, Wang X, Schwinn MK, Qin B, Long HW, Daniels DL, Hahn WC, Dowell RD, et al. HIF1A Employs CDK8-Mediator to Stimulate RNAPII Elongation in Response to Hypoxia. Cell. 2013; 153:1327–1339. [PubMed: 23746844]

Holstege FC, Jennings EG, Wyrick JJ, Lee TI, Hengartner CJ, Green MR, Golub TR, Lander ES, Young RA. Dissecting the regulatory circuitry of a eukaryotic genome. Cell. 1998; 95:717–728. [PubMed: 9845373]

Hurlin PJ, Steingrimsson E, Copeland NG, Jenkins NA, Eisenman RN. Mga, a dual-specificity transcription factor that interacts with Max and contains a T-domain DNA-binding motif. EMBO J. 1999; 18:7019–7028. [PubMed: 10601024]

Imhof A, Schuierer M, Werner O, Moser M, Roth C, Bauer R, Buettner R. Transcriptional regulation of the AP-2alpha promoter by BTEB-1 and AP-2rep, a novel wt-1/egr-related zinc finger repressor. Mol Cell Biol. 1999; 19:194–204. [PubMed: 9858544]

Jishage M, Malik S, Wagner U, Uberheide B, Ishihama Y, Hu X, Chait BT, Gnatt A, Ren B, Roeder RG. Transcriptional regulation by Pol II(G) involving mediator and competitive interactions of Gdown1 and TFIIF with Pol II. Mol Cell. 2012; 45:51–63. [PubMed: 22244332]

Kagey M, Newman J, Bilodeau S, Zhan Y, Van Berkum N, Orlando DA, Ebmeier CC, Goossens J, Rahl P, Levine S, et al. Mediator and Cohesin connect gene expression and chromatin architecture. Nature. 2010; 467:430–435. [PubMed: 20720539]

Kanin EI, Kipp RT, Kung C, Slattery M, Viale A, Hahn S, Shokat KM, Ansari AZ. Chemical inhibition of the TFIIH-associated kinase cdk7/kin28 does not impair global mRNA synthesis. Proc Natl Acad Sci U S A. 2007; 104:5812–5817. [PubMed: 17392431]

Khakhina S, Cooper KF, Strich R. Med13p prevents mitochondrial fission and programmed cell death in yeast through nuclear retention of cyclin C. Mol Biol Cell. 2014; 25:2807–2816. [PubMed: 25057017]

Knuesel MT, Meyer KD, Bernecky C, Taatjes DJ. The human CDK8 subcomplex is a molecular switch that controls Mediator co-activator function. Genes Dev. 2009; 23:439–451. [PubMed: 19240132]

Kuchin S, Yeghiayan P, Carlson M. Cyclin-dependent protein kinase and cyclin homologs SSN3 and SSN8 contribute to transcriptional control in yeast. Proc Natl Acad Sci U S A. 1995; 92:4006–4010. [PubMed: 7732022]

Kwak H, Lis JT. Control of transcriptional elongation. Ann Rev Genetics. 2013; 47:483–508. [PubMed: 24050178]

Lin C, Smith ER, Takahashi H, Lai KC, Martin-Brown S, Florens L, Washburn MP, Conaway JW, Conaway RC, Shilatifard A. AFF4, a component of the ELL/P-TEFb elongation complex and a shared subunit of MLL chimeras, can link transcription elongation to leukemia. Mol Cell. 2010; 37:429–437. [PubMed: 20159561]

Lindsay AK, Morales DK, Liu Z, Grahl N, Zhang A, Willger SD, Myers LC, Hogan DA. Analysis of Candida albicans mutants defective in the Cdk8 module of mediator reveal links between metabolism and biofilm formation. PLoS Genetics. 2014; 10:e1004567. [PubMed: 25275466]

Liu Y, Kung C, Fishburn J, Ansari AZ, Shokat KM, Hahn S. Two cyclin-dependent kinases promote RNA polymerase II transcription and formation of the scaffold complex. Mol Cell Biol. 2004; 24:1721–1735. [PubMed: 14749387]

Luo Z, Lin C, Shilatifard A. The super elongation complex (SEC) family in transcriptional control. Nat Rev Mol Cell Biol. 2012; 13:543–547. [PubMed: 22895430]

Margolin AA, Ong SE, Schenone M, Gould R, Schreiber SL, Carr SA, Golub TR. Empirical Bayes analysis of quantitative proteomics experiments. PLoS One. 2009; 4:e7454. [PubMed: 19829701]

Morin PJ, Sparks AB, Korinek V, Barker N, Clevers H, Vogelstein B, Kinzler KW. Activation of beta-catenin-Tcf signaling in colon cancer by mutations in beta-catenin or APC. Science. 1997; 275:1787–1790. [PubMed: 9065402]

Morris EJ, Ji J, Yang F, Di Stefano L, Herr A, Moon N, Kwon E, Haigis KM, Naar AM, Dyson NJ. E2F1 represses b-catenin transcription and is antagonized by both pRB and CDK8. Nature. 2008; 455:552–556. [PubMed: 18794899]

Mousley CJ, Yuan P, Gaur NA, Trettin KD, Nile AH, Deminoff SJ, Dewar BJ, Wolpert M, Macdonald JM, Herman PK, et al. A sterol-binding protein integrates endosomal lipid metabolism with TOR signaling and nitrogen sensing. Cell. 2012; 148:702–715. [PubMed: 22341443]

Nelson C, Goto S, Lund K, Hung W, Sadowski I. Srb10/Cdk8 regulates yeast filamentous growth by phosphorylating the transcription factor Ste12. Nature. 2003; 421:187–190. [PubMed: 12520306]

Pelish HE, Liau BB, Nitulescu II, Tangpeerachaikul A, Poss ZC, Da Silva DH, Caruso BT, Arefolov A, Fadeyi O, Christie AL, et al. Mediator kinase inhibition further activates super-enhancer-associated genes in AML. Nature. 2015; 526:273–276. [PubMed: 26416749]

Plaschka C, Lariviere L, Wenzeck L, Seizl M, Hemann M, Tegunov D, Petrotchenko EV, Borchers CH, Baumeister W, Herzog F, et al. Architecture of the RNA polymerase II-Mediator core initiation complex. Nature. 2015; 518:376–380. [PubMed: 25652824]

Raithatha S, Su TC, Lourenco P, Goto S, Sadowski I. Cdk8 regulates stability of the transcription factor Phd1 to control pseudohyphal differentiation of Saccharomyces cerevisiae. Mol Cell Biol. 2012; 32:664–674. [PubMed: 22124158]

Ritchie ME, Phipson B, Wu D, Hu Y, Law CW, Shi W, Smyth GK. limma powers differential expression analyses for RNA-sequencing and microarray studies. Nucleic Acids Res. 2015; 43:e47. [PubMed: 25605792]

Sanso M, Levin RS, Lipp JJ, Wang VY, Greifenberg AK, Quezada EM, Ali A, Ghosh A, Larochelle S, Rana TM, et al. P-TEFb regulation of transcription termination factor Xrn2 revealed by a chemical genetic screen for Cdk9 substrates. Genes Dev. 2016; 30:117–131. [PubMed: 26728557]

Sasaki T, Maier B, Koclega KD, Chruszcz M, Gluba W, Stukenberg PT, Minor W, Scrable H. Phosphorylation regulates SIRT1 function. PLoS One. 2008; 3:e4020. [PubMed: 19107194]

Sato S, Tomomori-Sato C, Parmely TJ, Florens L, Zybailov B, Swanson SK, Banks CAS, Jin J, Cai Y, Washburn MP, et al. A set of consensus mammalian mediator subunits identified by

multidimensional protein identification technology. Mol Cell. 2004; 14:685–691. [PubMed: 15175163]

Stuart SA, Houel S, Lee T, Wang N, Old WM, Ahn NG. A Phosphoproteomic Comparison of B-RAFV600E and MKK1/2 Inhibitors in Melanoma Cells. Mol Cell Proteomics. 2015; 14:1599–1615. [PubMed: 25850435]

Subramanian A, Tamayo P, Mootha VK, Mukherjee S, Ebert BL, Gillette MA, Paulovich A, Pomeroy SL, Golub TR, Lander ES, et al. Gene set enrichment analysis: a knowledge-based approach for interpreting genome-wide expression profiles. Proc Natl Acad Sci U S A. 2005; 102:15545–15550. [PubMed: 16199517]

Sundqvist A, Bengoechea-Alonso MT, Ye X, Lukiyanchuk V, Jin J, Harper JW, Ericsson J. Control of lipid metabolism by phosphorylation-dependent degradation of the SREBP family of transcription factors by SCF(Fbw7). Cell Metab. 2005; 1:379–391. [PubMed: 16054087]

Svaren J, Sevetson BR, Apel ED, Zimonjic DB, Popescu NC, Milbrandt J. NAB2, a corepressor of NGFI-A (Egr-1) and Krox20, is induced by proliferative and differentiative stimuli. Mol Cell Biol. 1996; 16:3545–3553. [PubMed: 8668170]

Szklarczyk D, Franceschini A, Wyder S, Forslund K, Heller D, Huerta-Cepas J, Simonovic M, Roth A, Santos A, Tsafou KP, et al. STRING v10: protein-protein interaction networks, integrated over the tree of life. Nucleic Acids Res. 2015; 43:D447–452. [PubMed: 25352553]

Taatjes DJ, Naar AM, Andel F, Nogales E, Tjian R. Structure, function, and activator-induced conformations of the CRSP coactivator. Science. 2002; 295:1058–1062. [PubMed: 11834832]

Takahashi H, Parmely TJ, Sato S, Tomomori-Sato C, Banks CA, Kong SE, Szutorisz H, Swanson SK, Martin-Brown S, Washburn MP, et al. Human Mediator subunit MED26 functions as a docking site for transcription elongation factors. Cell. 2011; 146:92–104. [PubMed: 21729782]

Ubersax JA, Ferrell JE Jr. Mechanisms of specificity in protein phosphorylation. Nat Rev Mol Cell Biol. 2007; 8:530–541. [PubMed: 17585314]

Wagschal A, Rousset E, Basavarajaiah P, Contreras X, Harwig A, Laurent-Chabalier S, Nakamura M, Chen X, Zhang K, Meziane O, et al. Microprocessor, Setx, Xrn2, and Rrp6 co-operate to induce premature termination of transcription by RNAPII. Cell. 2012; 150:1147–1157. [PubMed: 22980978]

Walker AK, Yang F, Jiang K, Ji JY, Watts JL, Purushotham A, Boss O, Hirsch ML, Ribich S, Smith JJ, et al. Conserved role of SIRT1 orthologs in fasting-dependent inhibition of the lipid/cholesterol regulator SREBP. Genes Dev. 2010; 24:1403–1417. [PubMed: 20595232]

Xu W, Wang Z, Zhang W, Qian K, Li H, Kong D, Li Y, Tang Y. Mutated K-ras activates CDK8 to stimulate the epithelial-to-mesenchymal transition in pancreatic cancer in part via the Wnt/beta-catenin signaling pathway. Cancer Lett. 2015; 356:613–627. [PubMed: 25305448]

Zhao X, Feng D, Wang Q, Abdulla A, Xie XJ, Zhou J, Sun Y, Yang ES, Liu LP, Vaitheesvaran B, et al. Regulation of lipogenesis by cyclin-dependent kinase 8-mediated control of SREBP-1. The J Clin Invest. 2012; 122:2417–2427. [PubMed: 22684109]

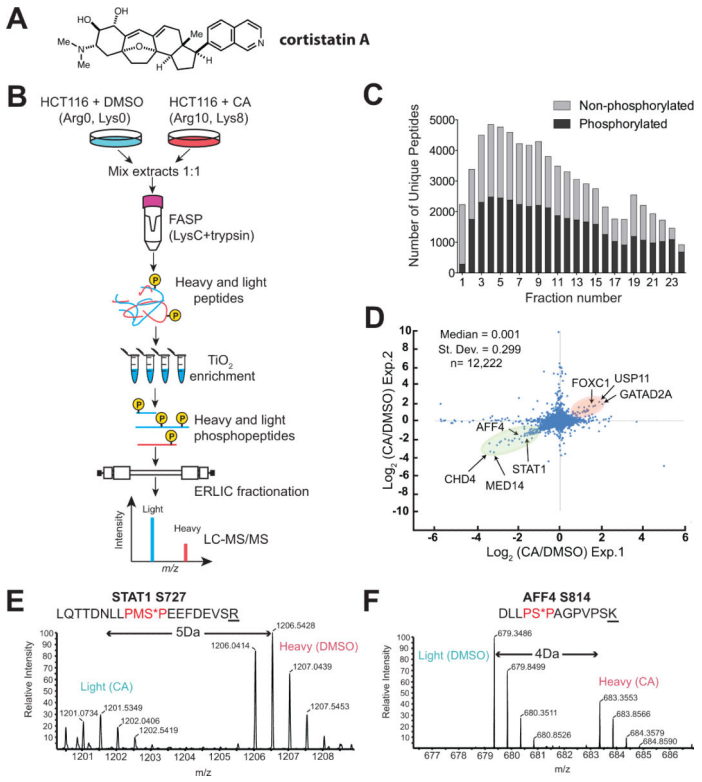

Figure 1. Quantitative phosphoproteomics in HCT116 cells ± CA

(A) Cortistatin A (CA) structure.

(B) Overview of phosphoproteomics workflow used to identify Mediator kinase substrates.

(C) Unique phosphopeptides identified with LC-MS/MS after ERLIC fractionation. Average of biological triplicates is represented.

(D) CA treatment with quantitative phosphoproteomics reproducibly identifies Mediator kinase substrates. H/L ratios quantified in two of three biological replicates are plotted on the x- and y- axes. Plot shows proteins whose H/L ratios decrease (green) and increase (peach) upon CA treatment.

(E) and (F) Representative mass spectra. Spectra shown are from replicates in which either the light (E) or heavy (F) cells were CA-treated. Differences in SILAC pairs are shown based on the labeled amino acid; Arg(10) in (E) and Lys(8) in (F). The charge is +2 for both peptides.

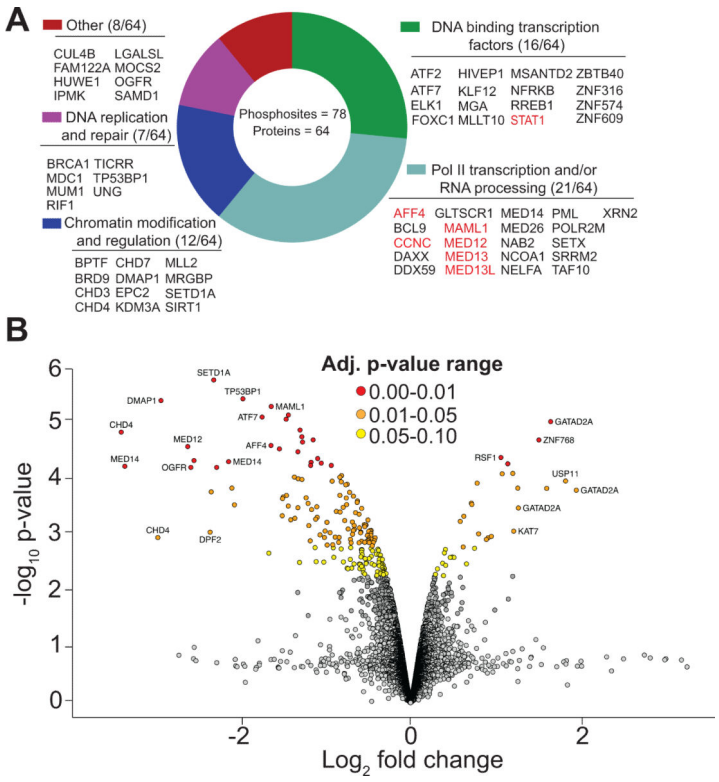

Figure 2. Identification of Mediator kinase (CDK8/19) substrates

(A) Functional categorization of high-confidence Mediator kinase substrates identified.

(B) Volcano plot of statistically significant phosphosite changes with CA treatment using an empirical Bayes analysis.

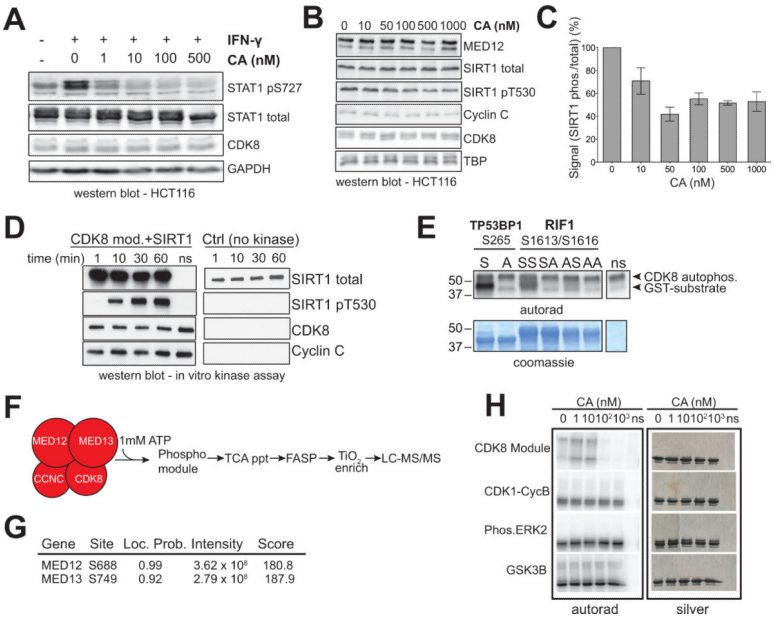

Figure 3. In vitro validation of select CDK8/19 substrates

(A) Validation of STAT1 S727 as a Mediator kinase target in HCT116 cells.

(B) Western blot validation of SIRT1 T530 as a Mediator kinase target. Levels of total SIRT1 and other proteins known to regulate CDK8 activity (MED12 or CCNC), remained unchanged. TBP is a loading control.

(C) Quantitation of data in (B). Error bars are SEM; n=2 for technical replicates.

(D) *In vitro* kinase assay with recombinant CDK8 module and SIRT1. With increasing time, SIRT1 pT530 detection increases, indicating CDK8 is phosphorylating this site. Increase is not seen in no kinase or no substrate (ns) controls.

(E) *In vitro* kinase assay with GST-tagged TP53BP1 or RIF1 fragments. Alanine mutations at identified phosphorylation sites show reduced phosphorylation by CDK8.

(F) Overview of method for identifying MED12 and MED13 phosphorylation sites using recombinant CDK8 modules.

(G) Verification of MED12 S688 and MED13 S749 phosphorylation sites.

(H) *In vitro* kinase assay using CA and GST-pol II CTD as a substrate. Whereas each kinase tested phosphorylates this substrate, CA only inhibits the CDK8 module.

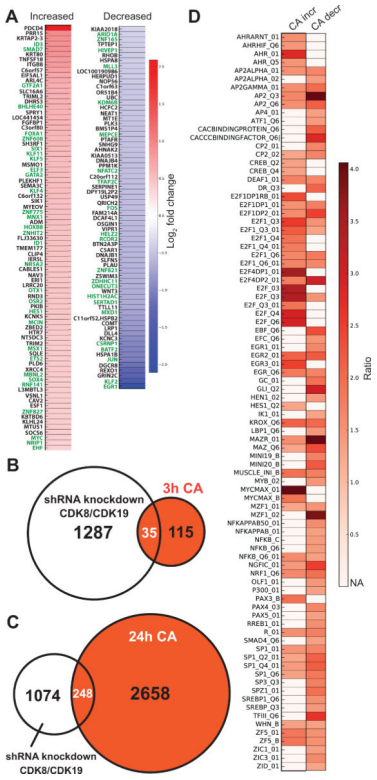

Figure 4. Mediator kinase inhibition is functionally distinct from CDK8 or CDK19 knockdown

(A) Heat map of differentially expressed genes (RNA-Seq) after 3 hr CA treatment. **Green font** represents transcription or chromatin regulator.

(B and C) Comparison with microarray data (Galbraith et al., 2013) using stable CDK8/19 knockdown (shRNA) vs. 3h CA treatment (B) or 24h treatment (C) in HCT116 cells under normal growth conditions. A 1.5-fold cutoff was used for microarray data and Cufflinks was used for CA-treated cells (no specific fold-change cutoff).

(D) TFBS analysis of promoters for genes whose expression changed with 3h CA treatment (listed in A). Promoters (±2kb from the TSS of the canonical isoform) were analyzed using F-Match, part of the Transfac database. Overrepresented sites with at least 1.5 fold increase vs. control promoters are shown for Transfac vertebrate matrices. Matrix name at left.

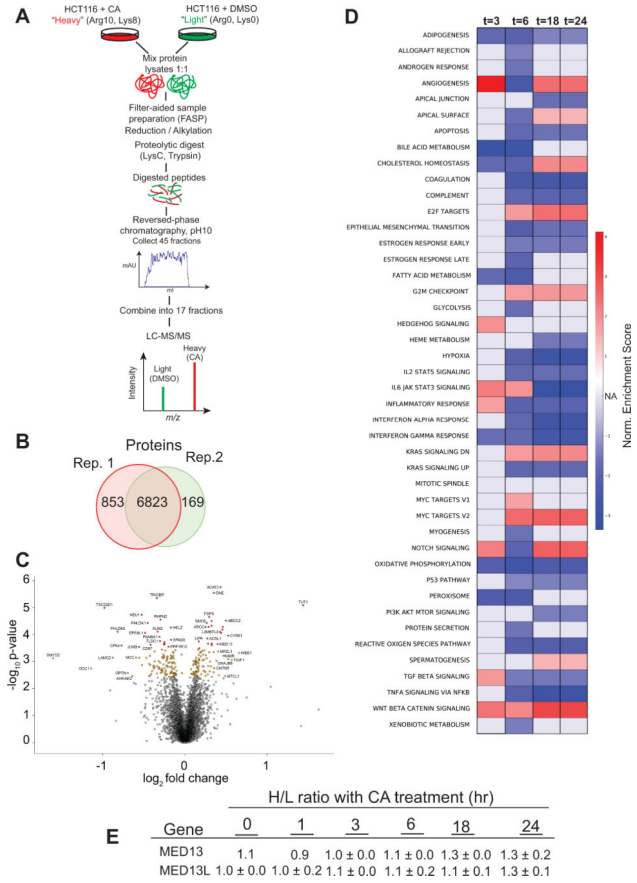

Figure 5. Quantitative proteomics reveals pathways and proteins affected by Mediator kinase inhibition

(A) Overview of quantitative proteomics method.

(B) Venn diagram of biological replicates showing number of proteins identified in the time series. Replicates show a high degree of overlap for protein IDs.

(C) Volcano plot comparing protein abundance at 18 hr and 24 hr time points vs. control (0 hr). Adjusted p-values are colored according to an empirical Bayes analysis.

(D) Individual analysis of t = 3hr, 6hr, 18hr, and 24hr CA treatment time points using GSEA and the hallmark gene sets from the Molecular Signatures Database. Comparison of the t = 0hr and 1hr time points showed no differences in the hallmark gene sets (not shown). The color of the heat map corresponds to the direction and magnitude of the normalized enrichment score for that gene set at each time point, compared to t = 0hr controls. ‘NA’ and the corresponding color indicate a hallmark gene set not being identified from the proteome data at the designated time.

(E) Protein abundance increases for MED13 and MED13L in CA-treated cells.

Table 1

High confidence Mediator kinase substrates identified using CA and quantitative phosphoproteomics

Protein ID	Gene Name	Position	Loc. Prob.	Ratio (H/L)	Adj. p-value
Q9UHB7	AFF4	S31	0.79	0.209 ± 0.011	0.025
Q9UHB7	AFF4	S32	0.78	0.248 ± 0.070	0.056
Q9UHB7	AFF4	S1043	1.00	0.325 ± 0.035	0.020
Q9UHB7	AFF4	S814	1.00	0.410 ± 0.012	0.018
P15336	ATF2	S136	1.00	0.366 ± 0.012	0.015
P17544	ATF7	S434	0.88	0.302 ± 0.020	0.015
P17544	ATF7	S111	0.75	0.590 ± 0.062	0.082
P17544	ATF7	T112	0.99	0.593 ± 0.019	0.036
O00512	BCL9	S291	0.95	0.694 ± 0.031	0.092
Q12830	BPTF	S1300	1.00	0.691 ± 0.035	0.095
P38398	BRCA1	S1613	0.96	0.447 ± 0.036	0.025
Q9H8M2	BRD9	S588	1.00	0.455 ± 0.009	0.019
H0YBQ5;E5RFK5	CCNC;CCNC	S218;S272	1.00	0.642 ± 0.037	0.066
Q12873	CHD3	S1601	1.00	0.595 ± 0.036	0.048
Q14839	CHD4	T1553	0.94	0.096 ± 0.002	0.018
Q9P2D1	CHD7	T2153	0.99	0.572 ± 0.024	0.034
K4DI93	CUL4B	S15	0.90	0.394 ± 0.038	0.078
Q9UER7	DAXX	S671	1.00	0.651 ± 0.014	0.053
Q5T1V6	DDX59	S64 / S76	0.99 / 0.76	0.535 ± 0.045	0.064
Q9NPF5	DMAP1	T409	1.00	0.134 ± 0.018	0.015
P19419	ELK1	S324	1.00	0.636 ± 0.058	0.092
Q52LR7	EPC2	T353	0.97	0.403 ± 0.019	0.059
Q96E09	FAM122A	S267	0.79	0.513 ± 0.082	0.085
Q12948	FOXC1	S241	1.00	0.433 ± 0.063	0.048
Q9NZM4	GLTSCR1	S755	1.00	0.394 ± 0.052	0.032
P15822	HIVEP1	S479	0.99	0.649 ± 0.019	0.055
Q7Z6Z7	HUWE1	S3816	0.98	0.527 ± 0.018	0.025
Q8NFU5	IPMK	S7	1.00	0.663 ± 0.050	0.098
Q9Y4C1	KDM3A	S445	1.00	0.448 ± 0.034	0.025
Q9Y4X4	KLF12	S202	1.00	0.441 ± 0.071	0.056
Q3ZCW2	LGALSL	S25	0.99	0.698 ± 0.029	0.092
Q92585	MAML1	S159	1.00	0.325 ± 0.009	0.015
Q92585	MAML1	S303	0.98	0.356 ± 0.018	0.049
Q14676	MDC1	S1775	1.00	0.453 ± 0.075	0.061
Q93074	MED12	S688	0.99	0.168 ± 0.036	0.020
Q9UHV7	MED13	S749	0.96	0.356 ± 0.041	0.073
Q71F56	MED13L	S878	1.00	0.568 ± 0.060	0.065

Protein ID	Gene Name	Position	Loc. Prob.	Ratio (H/L)	Adj. p-value
O60244	MED14	S1112	1.00	0.233 ± 0.045	0.025
O60244	MED14	S1128 / S1136	0.99 / 0.99	0.100 ± 0.015	0.025
O95402	MED26	S314	1.00	0.177 ± 0.039	0.025
Q8IWI9	MGA	S2924	0.99	0.660 ± 0.032	0.070
O14686	MLL2	S3199	0.98	0.630 ± 0.019	0.047
P55197	MLLT10	S346	1.00	0.470 ± 0.005	0.076
O96007	MOCS2	S20	1.00	0.531 ± 0.035	0.034
Q9NV56	MRGBP	S195	1.00	0.611 ± 0.023	0.043
Q6P1R3	MSANTD2	S27	1.00	0.623 ± 0.053	0.085
Q2TAK8	MUM1	S326	1.00	0.582 ± 0.050	0.059
Q15742	NAB2	S162	1.00	0.573 ± 0.014	0.032
Q15788	NCOA1	S698	1.00	0.381 ± 0.042	0.081
Q9H3P2	NELFA	S363	0.96	0.403 ± 0.032	0.023
Q9H3P2	NELFA	S360	0.50	0.441 ± 0.039	0.092
Q6P4R8	NFRKB	S1291	1.00	0.688 ± 0.035	0.092
Q9NZT2	OGFR	S349	1.00	0.170 ± 0.015	0.025
Q9NZT2	OGFR	S484	0.99	0.348 ± 0.035	0.021
P29590	PML	S530	1.00	0.674 ± 0.012	0.059
Q6EEV4	POLR2M	S10	0.99	0.416 ± 0.018	0.019
Q5UIP0	RIF1	S1613	0.98	0.357 ± 0.014	0.048
Q5UIP0	RIF1	S1616	1.00	0.418 ± 0.051	0.033
Q92766	RREB1	S1653	1.00	0.237 ± 0.025	0.039
Q6SPF0	SAMD1	S425	0.94	0.418 ± 0.022	0.019
O15047	SETD1A	T1088	1.00	0.204 ± 0.010	0.015
Q7Z333	SETX	S2612	1.00	0.465 ± 0.018	0.080
Q96EB6	SIRT1	T530	1.00	0.201 ± 0.030	0.043
Q9UQ35	SRRM2	S2449	1.00	0.708 ± 0.004	0.081
P42224	STAT1	S727	0.99	0.367 ± 0.001	0.047
Q12962	TAF10	S44	1.00	0.565 ± 0.020	0.032
Q7Z2Z1	TICRR	S1413	0.99	0.472 ± 0.066	0.059
Q12888	TP53BP1	S265	1.00	0.258 ± 0.014	0.015
Q12888	TP53BP1	S525	1.00	0.600 ± 0.014	0.036
P13051	UNG	S63	0.84	0.473 ± 0.026	0.025
P13051	UNG	T60 / S63	0.99 / 0.62	0.487 ± 0.027	0.025
Q9H0D6	XRN2	S487	1.00	0.566 ± 0.041	0.047
Q9NUA8	ZBTB40	T166	0.99	0.378 ± 0.078	0.058
A6NFI3	ZNF316	S10	1.00	0.598 ± 0.043	0.056
Q6ZN55	ZNF574	S717	1.00	0.406 ± 0.052	0.033
O15014	ZNF609	S804	1.00	0.373 ± 0.001	0.015

All sites correspond to reviewed accessions and canonical isoforms in Uniprot except for CCNC, whose identified site is not present in the canonical isoform. The ‘p-value’ column represents an adjusted p-value from an empirical Bayes analysis (Ritchie et al., 2015). See also **Supplemental Note**.